

## Utilization of molybdenum disulfide-graphene aerogel composite for hemoglobin-based electrochemical sensor for highly sensitive detection of bromate

Weili Zhang<sup>1\*</sup>, Chengkui Xiahou<sup>1</sup>, Xia Ji<sup>1</sup>, Yujun Zhang<sup>1</sup>, Hua Zhang<sup>1</sup>, Shuhuan Song<sup>2</sup>, Xueliang Niu<sup>2\*</sup>

<sup>1</sup>College of Pharmacy, Key Laboratory of Biomedical Engineering and Technology in Universities of Shandong, Qilu Medical University, Zibo 255300, PR China

<sup>2</sup>School of Chemistry and Chemical Engineering, Shandong University of Technology, Zibo 255049, P. R. China

\*E-mail: [23774989@qq.com](mailto:23774989@qq.com) (Weili Zhang), [xueliangniu@sdut.edu.cn](mailto:xueliangniu@sdut.edu.cn) (Xueliang Niu)

Received: 1 June 2022 / Accepted: 6 July 2022 / Published: 7 August 2022

Sensitive, reliable determination of bromate is highly significant and desirable in environmental monitoring field. Herein, molybdenum disulfide-graphene aerogel (MoS<sub>2</sub>-GA) is prepared by hydrothermal method, and further modified on glassy carbon electrode (GCE) to serve as a substrate for hemoglobin (Hb) immobilization. After the coating of PEDOT:PSS membrane, the Hb based sensing platform (PEDOT:PSS/Hb/MoS<sub>2</sub>-GA/GCE) is obtained. The direct electrochemistry of Hb is achieved, exhibiting a typical pair of obvious redox peaks. PEDOT:PSS/Hb/MoS<sub>2</sub>-GA/GCE displays outstanding electrocatalytic activity towards bromate reduction with catalytic mechanism discussed. Consequently, a sensitive electrochemical sensor for bromate determination is established, with a wide linear range from 1.0 μmol/L to 10.0 mmol/L, accompanying a low limit of detection (0.35 μmol/L). The sensor can be successfully applied for bromate detection in water samples with the characteristics of promising sensitivity, selectivity, and repeatability.

**Keywords:** PEDOT:PSS; Molybdenum disulfide; Graphene aerogel; Hemoglobin; Bromate; Electrochemical sensor

### 1. INTRODUCTION

The presence of small amount of chemical contaminants in drinking water can even have serious impact on human health [1]. Bromate is one member of oxyhalide, which can be produced as a by-product during the ozonation disinfection process of drinking water [2,3]. According to the research of the International Agency for Research on Cancer (IARC), bromate is a potential carcinogenic and genotoxic compound, which can induce cancerization in animal tissues and has been identified as a 2B

potential carcinogen [4]. The US Environmental Protection Agency (EPA) as well as the World Health Organization (WHO) standards for drinking water specify that the maximum allowable value of bromate is 10  $\mu\text{g/L}$  [4]. The excess level of bromate can cause damage to kidney, nervous system, renal cell tumors, and even genotoxicity [5]. Therefore, the accurate, sensitive determination of bromate in practical samples is highly desirable and great significant for human health. Up to now, various analytical approaches have been explored for bromate detection, such as spectrophotometry [6], ion chromatography [7] and electrochemical method [8, 9]. Among them, electrochemical approaches are widely explored for bromate determination owing to its uniform characteristics, such as simplicity, high sensitivity, fast analysis, low cost, and simultaneously can offer some information about the reaction mechanism of target on the electrode surface [10].

Recently, the third-generation electrochemical sensor on basis of the direct electrochemistry of metalloproteins or metalloenzymes has occupied much attention due to its high specificity and sensitivity [11, 12]. Hemoglobin (Hb), a low-cost and accessible metalloprotein, has been widely investigated and accepted as an ideal redox metalloprotein to construct electrochemical biosensors for its low cost and availability [13]. In the past few years, several Hb based biosensors have been explored for the determination of nitrite [14], trichloroacetic acid [15], hydrogen peroxide [16] and bromate [17]. However, to facilitate the direct electron transfer (DET) rate between Hb and electrode surface is still challenging because of the deeply buried prosthetic group in the protein shell [18]. To address this problem, novel two-dimensional and three-dimensional nanomaterials were induced to construct modified electrodes for Hb loading with the DET rate facilitated obviously [19, 20].

As a typical 2D material with outstanding chemical, electronic, catalytic, and biological properties,  $\text{MoS}_2$  has been applied in various fields such as catalysis [21], battery [22] and sensors [23].  $\text{MoS}_2$  displays high electrocatalytic activity for its rich active sites, and can be used as promising supporter in construction electrochemical biosensors as well for its high big surface area [24]. However, the poor conductivity restricted its electrochemical performance. Owing to the outstanding properties of large surface, abundant mesopores and rich channels, graphene aerogel (GA) has been accepted as a promising supporter for nanomaterials loading to form new nanocomposite [25].

Herein, the hybrid of  $\text{MoS}_2$  and GA ( $\text{MoS}_2$ -GA) was successfully synthesized. Furthermore, a novel Hb-based electrochemical biosensor for highly sensitive determination of bromate was constructed with  $\text{MoS}_2$ -GA modified glassy carbon electrode (GCE) sensing platform (PEDOT:PSS/Hb/ $\text{MoS}_2$ -GA/GCE). The DET of Hb in PEDOT:PSS/Hb/ $\text{MoS}_2$ -GA/GCE was achieved and accelerated greatly. Furthermore, Hb immobilized on the sensing platform displays strong electrocatalytic activity toward bromate reduction. The proposed biosensor evaluated by cyclic voltammetry provides a wider linear range, favorable stability and reproducibility toward bromate determination. The established Hb-based electrochemical sensor could be used for bromate analysis in practical water samples.

## 2. EXPERIMENTAL SECTION

### 2.1 Agents and instruments

Ammonium molybdate, thiourea, oxalic acid, PEDOT:PSS (1.3 wt%, Sinopharm Chemical Reagents Co., LTD. China), graphene oxide (GO, Tanmei Technology Co., China), bovine hemoglobin

(WM=68000, Koer Chemical, China), sodium bromate (Shanghai Chemical Reagent Factory, China) were purchased commercially and used directly.

All electrochemical experiments were performed using an electrochemical workstation (CHI600E, Shanghai Chenhua Co., LTD., China) with three-electrode system composed of the working electrode of modified GCE, the reference electrode of saturated calomel electrode (SCE) and the counter electrode of a platinum wire electrode. Scanning electron microscopy (SEM) images were recorded on a field emission scanning electron microscope (Apreos, FEI Company, America) at 20.0 kV.

## 2.2 Preparation of MoS<sub>2</sub>-GA nanocomposite

The synthesis procedure for MoS<sub>2</sub>-GA nanocomposite was designed according to previous work with some modifications [26, 27]. Briefly, 1.0 g ammonium molybdate and 1.6 g thiourea were dissolved with deionized water to 30 mL, denoted as solution A. Then 0.4 g oxalic acid was also dissolved in 30 mL deionized water, denoted as solution B. Solution A was slowly added to solution B within 30 minutes under magnetic stirring. Then 10 mL of the mixture was mixed with 10 mL of 2.0 mg/mL GO, and transferred to a 25 mL stainless steel high-pressure reactor, sealed, and heated at 200 °C for 20 hours. The composite was washed with ethanol and ultrapure water for several times, and then dried in a freeze dryer at -50°C for 12 hours. The obtained product was placed in a tubular furnace filled with an argon-hydrogen mixture (2% H<sub>2</sub>) atmosphere at an increase of 2°C to 450 °C per minute for 2 hours to get MoS<sub>2</sub>-GA nanocomposite. For comparison, MoS<sub>2</sub> was obtained according to the same procedure except the addition of GO.

## 2.3 Preparation of PEDOT:PSS/Hb/MoS<sub>2</sub>-GA/GCE

Prior to modification, the basic GCE was carefully polished with aluminum oxide powder ( $\phi=0.05\mu\text{m}$ ), then cleaned with ethanol and water under ultrasonic. After dried with pure N<sub>2</sub>, 6  $\mu\text{L}$  MoS<sub>2</sub>-GR (2.0 mg/L) was drip-coated on GCE surface to obtain MoS<sub>2</sub>-GA/GCE. Then 6  $\mu\text{L}$  Hb solution (15 mg/mL) was dropped on MoS<sub>2</sub>-GA/GCE. Finally, 6  $\mu\text{L}$  PEDOT:PSS solution was coated on Hb/MoS<sub>2</sub>-GA/GCE for fixation and preservation of Hb, after being dried naturally, the PEDOT:PSS/Hb/MoS<sub>2</sub>-GA/GCE was successfully fabricated and stored in refrigerator at 4 °C when free of use. Other modified electrodes were also prepared by the same method for comparison.

# 3. RESULTS AND DISCUSSION

## 3.1 Characterization of MoS<sub>2</sub>-GA nanocomposite

The microstructure of MoS<sub>2</sub>-GA nanocomposite was observed (Fig. 1A) by scanning electron microscope (SEM). As shown in Fig. 1B, the prepared MoS<sub>2</sub>-GA nanocomposite is a porous structure with MoS<sub>2</sub> in its typical nanoflower-like structure [28]. The formation of interconnected porous structure may be attributed to the highly folded reduced graphene oxide. It not only enhances the charge transfer

pathway in electrode reaction, but also provides a certain environment for MoS<sub>2</sub> growth, and oxygen-containing functional groups to bind MoS<sub>2</sub> precursors. There are a large number of pores in the composite, which increase the specific surface area, which supplies an excellent matrix for Hb immobilization. Meanwhile, it also provides a good reaction environment for the DET of Hb and the electrochemical reduction of bromate.

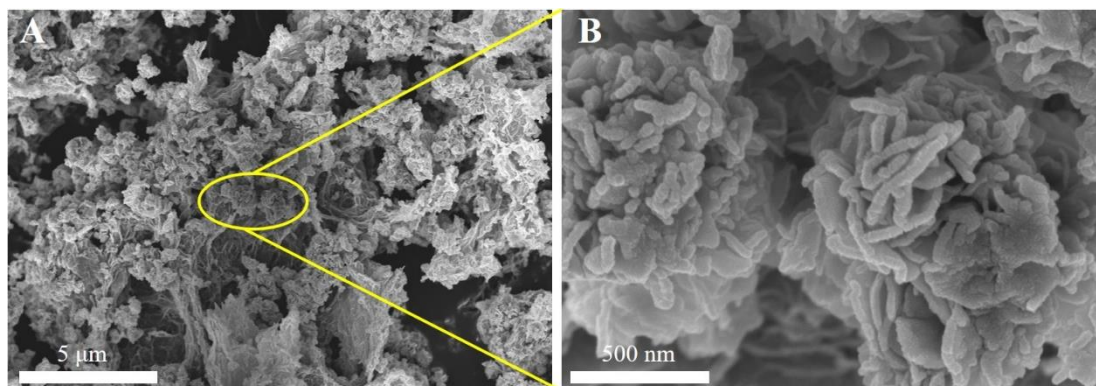


**Figure 1.** SEM images of MoS<sub>2</sub>-GA nanocomposite in a low (A) and high (B) amplified views.

### 3.2 Electrochemical performance of different electrodes

Fig. 2 shows the cyclic voltammetry (CV) curves of various electrodes 0.1 mol/L KCl solution containing 1.0 mmol/L [Fe(CN)<sub>6</sub>]<sup>3-/4-</sup>.

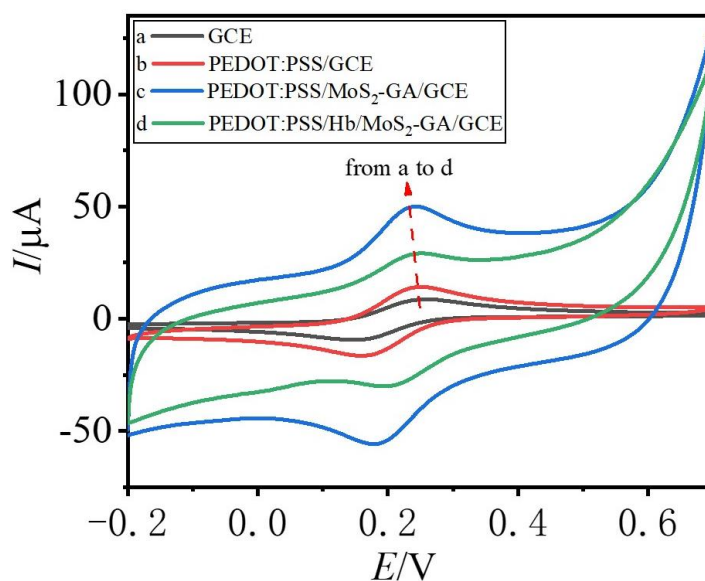


**Figure 2.** (A) CV curves of various modified electrodes (scan rate, 100 mV/s).

A pair of obvious quasi-reversible redox peaks appears on GCE, and the redox currents increase on PEDOT:PSS/GCE because the presence of conductive polymer film PEDOT:PSS accelerates electron transfer. The peak currents on PEDOT:PSS/MoS<sub>2</sub>-GA/GCE are further increased. Due to the large specific surface area, excellent electrical conductivity and abundant pore structure, MoS<sub>2</sub>-GA nanocomposite provides rich channels for mass and electron transfer of [Fe(CN)<sub>6</sub>]<sup>3-/4-</sup>. While on PEDOT:PSS/Hb/MoS<sub>2</sub>-GA/GCE, the peak current decreases for the poor conductivity of Hb, impeding the electron transfer of [Fe(CN)<sub>6</sub>]<sup>3-/4-</sup>.

### 3.3 Direct electrochemical behavior of Hb

The CV curves of different modified electrodes in pH 7.0 PBS buffer solution are shown in Fig. 3. No obvious Faraday currents can be observed on GCE (curve a), PEDOT:PSS/GCE (b) and PEDOT:PSS/MoS<sub>2</sub>-GA/GCE (curve c), indicating that no electrochemical reaction occurs within the scanning potential range. However, due to the presence of PEDOT:PSS, a interface double electric layer is formed, which makes the background current of PEDOT:PSS/GCE increase obviously. The background current of PEDOT:PSS/MoS<sub>2</sub>-GA composite is further increased and present polarization when the potential exceeds 0.0 V (vs. Ag/AgCl). After immobilization of Hb, PEDOT:PSS/Hb/GCE has an obvious reduction peak (curve d), indicating that an irreversible redox reaction of Hb occurred. As for PEDOT:PSS/Hb/MoS<sub>2</sub>-GA/GCE, a pair of symmetrical redox peaks appeared at -0.28 V and -0.43 V with the peak currents significantly enhanced. The pair of peaks is the characteristic peaks of the redox group of Fe(III)/Fe(II) buried in Hb molecular [29,30]. It indicates that the presence of MoS<sub>2</sub>-GA as membrane can improve the electron transfer rate between Hb and electrode. This is because that MoS<sub>2</sub>-GA has a porous structure and a large specific surface area, which can load more Hb and act as a bridge for direct electron transfer between Hb and electrode, thus speeding up the electron transfer rate. Therefore, MoS<sub>2</sub>-GA can provide a suitable microenvironment for the DET of Hb.

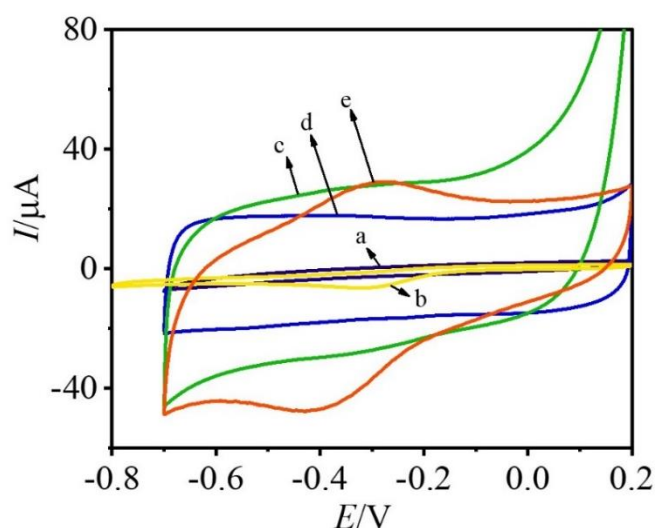


**Figure 3.** Cyclic voltammetry curves of different electrodes in the PB solution. GCE (a), PEDOT:PSS/GCE (b), PEDOT:PSS/MoS<sub>2</sub>-GA/GCE (c), PEDOT:PSS/Hb/GCE (d), and PEDOT:PSS/Hb/MoS<sub>2</sub>-GA/GCE (e).

### 3.4 Acidity effect on the DET of Hb

The influence of PBS acidity ranging from pH 5.0 to 8.0 was studied by CV technique. As shown in Fig. 4A, with the increase of pH value, the redox peak potentials moved to negatively, indicating the involvement of proton in the redox electrochemical process between Hb and electrode. There is a good linear relationship between  $E^{0'}$  and pH value with the regression equation as  $E^{0'} \text{ (V)} = -0.0454 \text{ pH} + 0.0181$  ( $\gamma = 0.998$ ). The slope value of  $-45.4 \text{ mV/pH}$  is close to the theoretical value of  $-59.0 \text{ mV/pH}$  (298K), demonstrating that there are equal number of proton and electron taking part to the electrode reaction. Consequently, the electrochemical reaction mechanism can be expressed as:  $\text{Hb Heme Fe (III)} + \text{H}^+ + \text{e}^- \rightarrow \text{Hb Heme Fe (II)}$  [31].

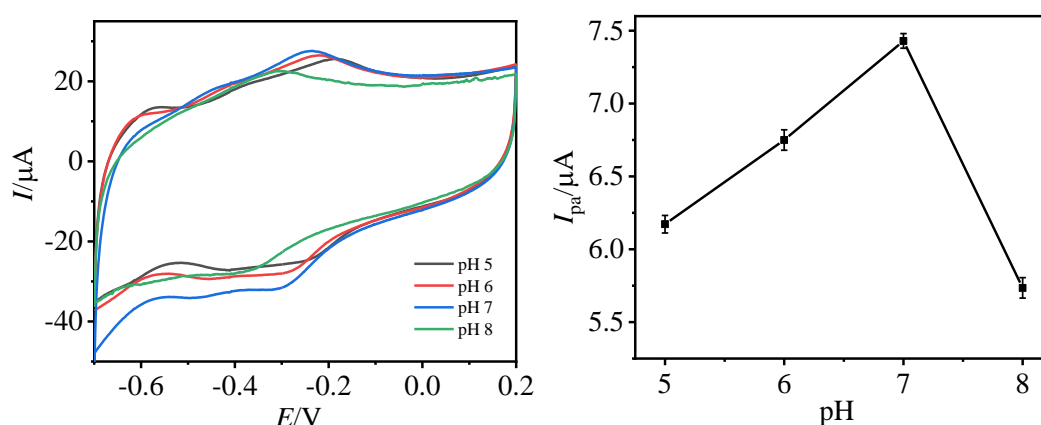


**Figure 4** (A) CVs of PEDOT:PSS/Hb/MoS<sub>2</sub>-GA/GCE in PBS with pH from 5.0 to 8.0 at a scan rate of 100 mV/s, (B) plot of  $I_{pa}$  vs. pH values.

As shown in Fig. 4B, the maximum value of oxidation peak current ( $I_{pa}$ ) appeared while the pH is 7.0. To obtain optimal sensitivity, pH 7.0 was selected as the buffer acidity for following investigations.

### 3.5 Effect of scanning speed on the DET of Hb

The electrochemical effect of sweep rate ( $v$ ) on the DET of Hb immobilized in PEDOT:PSS/Hb/MoS<sub>2</sub>-GA/GCE was studied. As the overlapped CV curves shown in Fig. 5A, with the increase of sweep speed from 0.03 to 0.9 V/s, the redox peak currents increase gradually as well as the oxidation and reduction peak potentials moves positively and negatively, respectively. The redox peak currents have good linear relationships with scanning rate (Fig. 5B) with linear regression equations as  $I_{pc} \text{ (A)} = -59.74 v \text{ (V/s)} - 1.76$  ( $\gamma = 0.998$ ),  $I_{pa} \text{ (}\mu\text{A)} = 42.48 v \text{ (V/s)} + 2.69$  ( $\gamma = 0.995$ ), indicating a typical surface controlled thin layer electrochemical behavior of the redox of PEDOT:PSS/Hb/MoS<sub>2</sub>-GA/GCE.

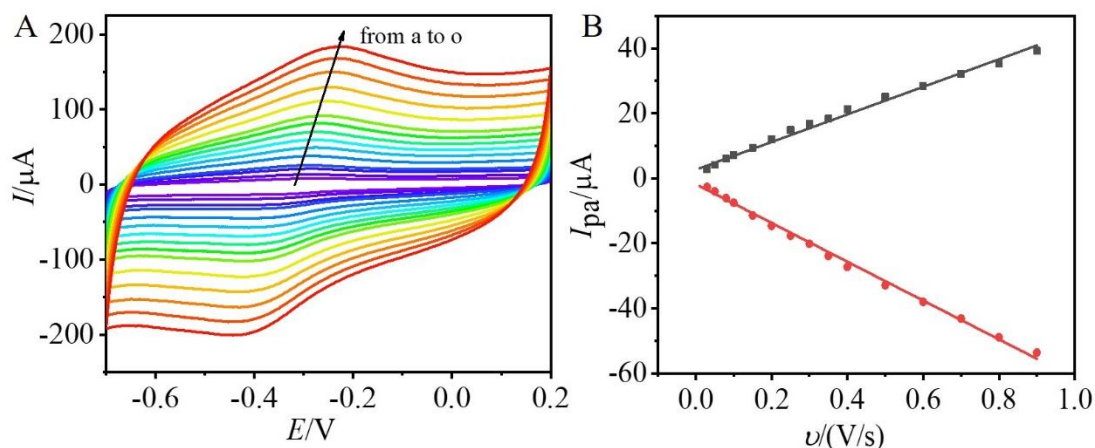


**Figure 5** (A) CV curves of PEDOT:PSS/Hb/MoS<sub>2</sub>-GA/GCE in pH 7.0 PBS with various scanning speeds (from “a” to “o” is 30, 50, 80, 100, 150, 200, 250, 300, 350, 400, 500, 600, 700, 800, 900 mV/s); (B) Linear relationships of peak currents versus scanning speeds ( $v$ ).

According to the formula  $Q=nFA\Gamma^*$  [32], where  $\Gamma^*$  is the surface concentration of the electroactive substance,  $n$  is the electron transfer number,  $F$  is the Faraday constant,  $A$  is the area of the electrode, and  $Q$  is the integral charge. The average surface coverage ( $\Gamma^*$ ) of electroactive Hb on the modified electrode was estimated to be  $1.61\times 10^{-9}$  mol/cm<sup>2</sup>, and the total amount fixed on the electrode surface is calculated as  $1.87\times 10^{-8}$  mol/cm<sup>2</sup>. Therefore, 8.61% of Hb molecules on the electrode surface were involved in the electrode reaction.

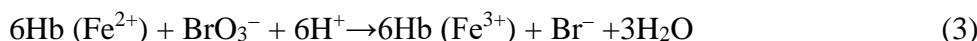
The  $\Delta E_p$  was got as 131 mV at sweep speed of 0.1 V/s, so  $n\Delta E_p$  is less than 200 mV. According to the Laviron theory [33],

$$m = (RT/F)(k_s/nv) \quad (1)$$

where  $m^{-1}$  is given as 0.14 by assuming  $\alpha=0.5$ , so  $k_s$  was calculated  $0.65 \text{ s}^{-1}$ , indicating that the existence of MoS<sub>2</sub>-GR can provide a suitable microenvironment for Hb with electron transfer accelerated.

### 3.6 Electrocatalytic performance of PEDOT:PSS/Hb/MoS<sub>2</sub>-GA/GCE

The electrocatalytic performance of PEDOT:PSS/Hb/MoS<sub>2</sub>-GA/GCE toward bromate reduction was investigated by CV technique in pH 7.0 PBS containing  $2\times 10^{-3}$  mol/L sodium bromate. The CV curves of PEDOT:PSS/MoS<sub>2</sub>-GA/GCE (curve a) and PEDOT:PSS/Hb/MoS<sub>2</sub>-GA/GCE (curve b) were shown in Fig. 6. By comparing the two electrodes, the electrocatalytic peak of Hb toward the reduction of bromate can be obviously observed at 0.60 V. The results show that PEDOT:PSS/Hb/MoS<sub>2</sub>-GA/GCE has outstanding electrocatalytic activity for bromate reduction. Based on the previous work [17], the electrocatalytic mechanism of Hb toward bromate reduction can be expressed as follows.



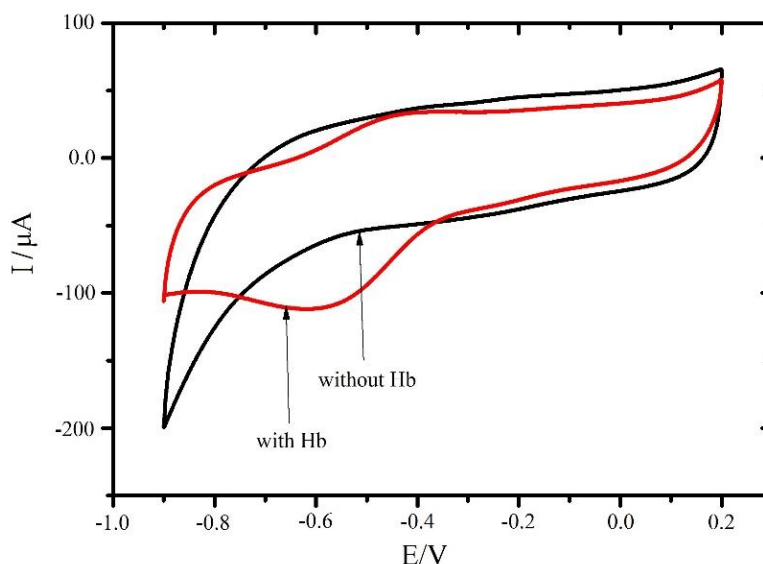


**Figure 6.** CV curves of PEDOT:PSS/Hb/MoS<sub>2</sub>-GA/GCE and PEDOT:PSS/ MoS<sub>2</sub>-GA/GCE in pH 7.0 PBS containing  $2 \times 10^{-3}$  mol/L sodium bromate.

The electrocatalytic performance of PEDOT:PSS/Hb/MoS<sub>2</sub>-GA/GCE toward bromate reduction at different concentrations was studied. With the increase of bromate amount, the reduction peak current increased significantly while the oxidation peak decreased gradually (Fig. 7A). The reduction peak current ( $I$ ) of Hb increased with bromate concentration from  $1.0 \times 10^{-3}$  to 10.0 mmol/L, obeying the linearly regression equation (Fig. 7B). The limit of detection (LOD) was calculated as  $0.35 \mu\text{mol/L}$  ( $3S_0/S$ ). The comparison of the proposed sensor with similar bromate sensors described in recent literature was listed in the following table 1. We can see that this novel PEDOT:PSS/Hb/MoS<sub>2</sub>-GA/GCE shows wider linear range and lower LOD, indicating a promising and reliable electrochemical sensor for highly sensitive determination of bromate.

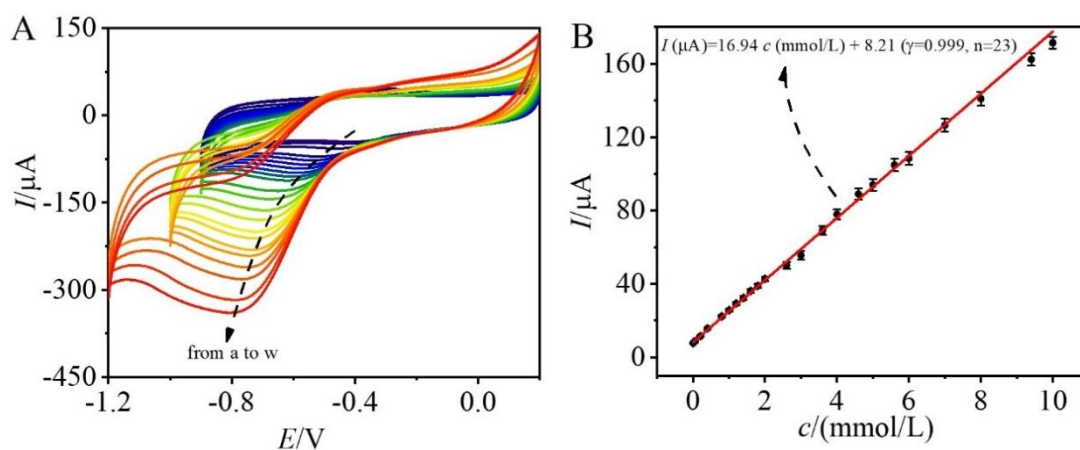


**Figure 7.** (A) CV curves of PEDOT:PSS/Hb/MoS<sub>2</sub>-GA/GCE in PBS containing sodium bromate with the concentration ranging from  $1 \times 10^{-6}$  to  $1.0 \times 10^{-2}$  mol/L at scanning rate of 100 mV/s. (B) Linear relationship between  $I$  and bromate concentration ( $n=3$ ).



**Table 1** Comparison of analytical performance of the fabricated PEDOT:PSS/Hb/MoS<sub>2</sub>-GA/GCE with some reported results for bromate determination.

Electrode*	Linear range (mmol/L)	LOD ( $\mu$ mol/L)	Refs.
Hb/f-MWCNT–P-L-His–ZnO/GCE	$2.0 \times 10^{-3}$ –15	0.30	[17]
Pd/MWNT/GCE	$0.1$ – $4.0 \times 10^4$	10.0	[34]
PANI-POMs/GCE	$7.5$ – $4.0 \times 10^2$	3.0	[35]
ERGO-PANOA-Pd/GCE	$4.0 \times 10^{-3}$ –0.84	1.0	[36]
FAD-modified SiO <sub>2</sub> /ZrO <sub>2</sub> /C ceramic electrode	$4.9 \times 10^{-2}$ –1.2	2.3	[37]
PEDOT:PSS/Hb/MoS <sub>2</sub> -GA/GCE	$1.0 \times 10^{-3}$ –10.0	0.35	This work

\*f-MWCNT, functionalized multiwalled carbon nanotubes; P-L-His Poly-L-Histidine; MWCNT, multiwalled carbon nanotubes; (PANI)-polyoxometalates (POM = XM<sub>12</sub>, X = P, Si and M = Mo, W); ERGO-PANOA-Pd, electrochemical reduced graphene oxide/poly(aniline-*co-o*-aminophenol)/palladium; FAD, flavin adenine dinucleotide.

### 3.7. Repeatability, stability and reproducibility

Ten times consecutive measurements were performed in pH 7.0 PBS containing 1.0 mmol/L bromate on one PEDOT:PSS/Hb/MoS<sub>2</sub>-GA/GCE with RSD as 3.85%, indicating good repeatability. The reduction peak current still maintains 97.8% of the original value after continuous scanning for 20 cycles. After continuous scanning for 50 cycles, the peak current decreased by 6.7 % compared with the original value. These results indicate that PEDOT:PSS/Hb/MoS<sub>2</sub>-GA/GCE has good stability. The peak current of PEDOT:PSS/Hb/MoS<sub>2</sub>-GA/GCE kept 95.3% after two weeks storage in 4 °C refrigerator, demonstrating promising stability, which could be attributed to the excellent biocompatibility of MoS<sub>2</sub>-GA nanocomposite, supplying a suitable microenvironment for Hb. Five parallelly fabricated PEDOT:PSS/Hb/MoS<sub>2</sub>-GA/GCEs were used to monitor 1.0 mmol/L bromate in PBS with a RSD of 5.6%, implying good reproducibility.

### 3.8 Sample analysis

The real application of PEDOT:PSS/Hb/MoS<sub>2</sub>-GA/GCE was evaluated by detecting bromate content in water samples.

**Table 2.** Bromate content detected in water samples with PEDOT:PSS/Hb/MoS<sub>2</sub>-GA/GCE (n =3).

Sample	Detected (mmol/L)	Added (mmol/L)	Detected (mmol/L)	Recovery (%)	RSD (%)
Tap water	\	0.100	0.095	95.0	3.5
		0.500	0.506	102	3.2
		1.000	1.040	104	2.7
Drinking water	\	0.100	0.097	97.0	4.2
		0.500	0.490	98.4	2.8
		1.000	1.030	103	3.3

The recoveries of bromate in different water samples were calculated by standard addition method with the results shown in Table 2. It demonstrates that no bromate was detected in any testing samples. The average recoveries of bromate was between 95.0 %~104% for tap water sample and 97.0 ~103% for drinking water sample with RSD less than 5.0 %, indicating reliable application of this electrochemical sensor for bromate determination in real samples.

#### 4. CONCLUSION

In this study, MoS<sub>2</sub>-GA shows a promising substrate for Hb immobilization on GCE. With coating PEDOT:PSS membrane, a new Hb based electrochemical sensor of PEDOT:PSS/Hb/MoS<sub>2</sub>-GA/GCE was constructed. The direct electrochemistry of Hb in PEDOT:PSS/Hb/MoS<sub>2</sub>-GA/GCE was successfully achieved with signals significantly enhanced. PEDOT:PSS/Hb/MoS<sub>2</sub>-GA/GCE displays outstanding electrocatalytic ability towards bromate reduction with catalytic mechanism discussed. Consequently, a novel electrochemical sensing method was proposed and could be successfully used for bromate detection in practical samples.

#### ACKNOWLEDGEMENTS

This work was financially supported by the Shandong Provincial Natural Science Foundation, China (ZR2021MB103); Project of Shandong Province Higher Educational Science and Technology Program (J18KA099) and Zibo Platform for Gene Editing and Cell Application (2019GECA013).

#### References

1. J. Marák, A. Staňová, V. Vaváková, M. Hrenáková and D. Kaniansky, *J. Chromatogr. A*, 1267 (2012) 252
2. U. Von Gunten and J. Hoigne, *Environ. Sci. Technol.*, 28 (1994) 1234
3. M. Saraji, N. Khaje and M. Ghani, *Microchim. Acta*, 181 (2014) 925
4. R. Mao, X. Zhao, H. Lan, H. Liu and J. Qu, *Water Res.*, 77 (2015) 1
5. J. Zhang and X. Yang, *Analyst*, 138 (2013) 434
6. L. Romele, *Analyst*, 123 (1998) 291
7. M. Ye, P. N. Nesterenko, Y. Lu, X. Huang and M. Chen, *J. Chromatogr. Sci.*, 58 (2020) 1
8. Y. Zhang, F. Wen, Y. Jiang, L. Wang, C. Zhou and H. Wang, *Electrochim. Acta*, 115 (2014) 504
9. T. Tamiji, A. Nezamzadeh-Ejhi, *J. Solid State Electr.*, 23 (2019) 143
10. S.A. Balogun, and O.E. Fayemi, *Biosensors*, 11 (2021) 172
11. Zou, R., X. Li, G. Luo, Y. Niu, W., Weng, W. Sun, J. Xi, Y. Chen and G. Li, *Electroanalysis*, 31 (2019) 575
12. X. Niu, H. Xie, G. Luo, Y. Men, W. Zhang and W. Sun, *J. Electrochem. Soc.*, 165 (2018) B713
13. K. K. Hussain, J. M. Moon, D. S. Park and Y. B. Shim, *Electroanalysis*, 29 (2017) 2190
14. J. Jiang, W. Fan and X. Du, *Biosens. Bioelectron.*, 51C (2014) 343
15. X. Li, X. Niu, W. Zhao, W. Chen, C. Yin, Y. Men, G. Li and W. Sun, *Electrochem. Commun.*, 86 (2017) 68-71.
16. D. Shan, G. Cheng, D. Zhu, H. Xue, S. Cosnier and S. Ding, *Sensor. Actuat. B Chem.*, 137 (2017) 259
17. A.T. Ezhil Vilian, S. Chen, C. H. Kwak, S.K. Hwang, Y. S. Huh and Y.K. Han, *Sensor. Actuat. B*

- Chem.*, 224 (2016) 607
18. S. Palanisamy, Y. Wang, S. Chen, B. Thirumalraj and B.S. Lou, *Microchim. Acta*, 183 (2016) 1953
  19. W. Sun, S. Gong, F. Shi, L. Cao, L. Ling, W. Zheng and W. Wang, *Mater. Sci.Eng. C*, 40 (2014) 235
  20. L. Hui, S. Xing, C. Duan, X. Dong and Z. Zhu, *Mater. Lett.*, 122 (2014) 182
  21. X. Zhang, F. Jia and S. Song, *Chem. Eng. J.*, 405 (2020) 127013
  22. J. Wu, F. Ciucci and J.K. Kim, *Chem. Eur. J.*, 26 (2020) 6296
  23. V. Yadav, S. Roy, P. Singh, Z. Khan and A. Jaiswal, *Small Methods*, 15 (2019) 1803706
  24. A.T.E. Vilian, B. Dinesh, S.M. Kang, U.M. Krishnan, Y.S. Huh and Y.K. Han, *Microchim. Acta*, 186 (2019) 203
  25. Q. Xu, H. Jia, X. Duan, L. Lu, Q. Tian, S. Chen, J. Xu and F. Jiang, *Inorg. Chem. Commun.*, 119 (2020) 108122
  26. G. Feng, A. Wei, Y. Zhao and J. Liu, *J. Mater. Sci: Mater. El*, 26 (2015) 8160
  27. K.S. Yu, X. Xu, C. Li and G. Shi, *ACS Nano*, 4 (2010) 4324
  28. Y. Shu, W. Zhang, H. Cai, Y. Yang, X. Yu and Q. Gao, *Nanoscale*, 11 (2019) 6644
  29. W. Sun, Y. Guo, X. Ju, Y. Zhang, X. Wang and Z. Sun, *Biosens. Bioelectron.*, 42 (2013) 207
  30. P. Li, Y. Ding, Z. Lu, Y. Li, X. Zhu, Y. Zhou, Y. Tang, Y. Chen, C. Cai and T. Lu *Talanta*, 115 (2013) 228
  31. X. Han, W. Huang, J. Jia, S. Dong and E. Wang, *Biosens. Bioelectron.*, 17 (2002) 741
  32. A.J. Bard and L.R. Faulkner, *Electrochemical Methods: Fundamentals and Applications*, Wiley, New York, 1980.
  33. E. Laviron, *J. Electroanal. Chem.*, 101(1979) 19
  34. D. Zhou, L. Ding, H. Cui, H. An, J. Zhai and Q. Li, *Chem. Eng. J.*, 200–202 (2012) 32
  35. G.G. Papagianni, D.V. Stergiou, G.S. Armatas, M.G. Kanatzidis and M.I. Prodromidis, *Sensor. Actuat. B: Chem.*, 173 (2012) 346
  36. Y. Zhang, F. Wen, Y. Jiang, L. Wang, C. Zhou and H. Wang, *Electrochim. Acta*, 115 (2014) 504
  37. E. Marafon, L.T. Kubota, Y. Gushikem, *J. Solid State Electrochem.*, 13 (2009) 377